Functional and morphological assessment of a standardized rat sciatic nerve crush injury with a non-serrated clamp

Varejao, A.S.P.; Cabrita, A.M.; Meek, M.F.; Bulas-Cruz, J.; Melo-Pinto, P.; Raimondo, S.; Geuna, S.; Giacobini-Robecchi, M.G.

Published in:
Journal of Neurotrauma

DOI:
10.1089/neu.2004.21.1652

JOURNAL OF NEUROTRAUMA
Volume 21, Number 11, 2004

Pp. 1652–1670

Functional and Morphological Assessment of a Standardized Rat Sciatic Nerve Crush Injury with a Non-Serrated Clamp

ARTUR S.P. VAREJÃO,[1] ANTÓNIO M. CABRITA,[2] MARCEL F. MEEK,[3] JOSÉ BULAS-CRUZ,[4] PEDRO MELO-PINTO,[4] STEFANIA RAIMONDO,[5] STEFANO GEUNA,[5] and MARIA G. GIACOBINI-ROBECCHI[5]

ABSTRACT

Peripheral nerve researchers frequently use the rat sciatic nerve crush as a model for axonotmesis. Unfortunately, studies from various research groups report results from different crush techniques and by using a variety of evaluation tools, making comparisons between studies difficult. The purpose of this investigation was to determine the sequence of functional and morphologic changes after an acute sciatic nerve crush injury with a non-serrated clamp, giving a final standardized pressure of $p = 9$ MPa. Functional recovery was evaluated using the sciatic functional index (SFI), the extensor postural thrust (EPT) and the withdrawal reflex latency (WRL), before injury, and then at weekly intervals until week 8 postoperatively. The rats were also evaluated preoperatively and at weeks 2, 4, and 8 by ankle kinematics, toe out angle (TOA), and gait-stance duration. In addition, the motor nerve conduction velocity (MNCV) and the gastrocnemius-soleus weight parameters were measured just before euthanasia. Finally, structural, ultrastructural and histomorphometric analyses were carried out on regenerated nerve fibers. At 8 weeks after the crush injury, a full functional recovery was predicted by SFI, EPT, TOA, and gait-stance duration, while all the other parameters were still recovering their original values. On the other hand, only two of the histomorphometric parameters of regenerated nerve fibers, namely myelin thickness/axon diameter ratio and fiber/axon diameter ratio, returned to normal values while all other parameters were significantly different from normal values. The employment of traditional methods of functional evaluation in conjunction with the modern techniques of computerized analysis of gait and histomorphometric analysis should thus be recommended for an overall assessment of recovery in the rat sciatic nerve crush model.

Key words: axonotmesis; computerized gait analysis; crushed peripheral nerve; functional recovery; morphologic studies; rat sciatic nerve

[1]Department of Veterinary Sciences, CETAV, University of Trás-os-Montes e Alto Douro, Vila Real, Portugal.
[2]Institute of Experimental Pathology, CHPEBD, Faculty of Medicine, Coimbra, Portugal.
[3]Department of Plastic Surgery, University Hospital Groningen, Groningen, The Netherlands.
[4]Department of Engineering, CETAV, University of Trás-os-Montes e Alto Douro, Vila Real, Portugal.
[5]Department of Clinical and Biological Sciences, University of Turin, Italy.

INTRODUCTION

NERVE CRUSH INJURY is a well-established axonotmetic model in experimental regeneration studies to investigate the impact of various pharmacological treatments (Al Moutaery et al., 1998; Algora et al., 1996; Gudemez et al., 2002; Islamov et al., 2002; Lee et al., 2000; Paydarfar and Paniello, 2001). It is relatively inexpensive, easy to handle, and the capacity for regeneration is equivalent in rats and subhuman primates (Mackinnon et al., 1985). Investigators have described several assessment parameters to measure neural regeneration. However, a poor correlation between the different techniques to evaluate peripheral nerve regeneration is frequently observed (Dellon and Mackinnon, 1989; Kanaya et al., 1996; Shen and Zhu, 1995).

The goals of this axonotmetic study were to describe the temporal sequence of functional recovery as predicted by a variety of motor and sensory tests and relate them with well estbalished morphological parameters. For this purpose, to evaluate the functional outcome after crush injury traditional methods such as the sciatic functional index (SFI), extensor postural thrust (EPT), the withdrawal reflex latency (WRL), the motor nerve conduction velocity (MNCV), and the gastrocnemius and soleus muscle weight were used. Additionally, the biomechanical behavior of the foot and ankle complex was investigated during the stance phase of walking. Recently, the study of some biomechanical parameters have given valuable insight into the effect of the sciatic denervation, and thus represents an integration of the neural control acting on the ankle and foot muscles (Varejão et al., 2003a,b). In addition, the morphological features of regenerated nerves were assessed at week 2 and week 8 post-crush, and a histomorphometrical analysis was carried out on regenerated myelinated nerve fibers.

Despite the axonotmetic lesion being a commonly used experimental model in the rat, there is an unfortunate lack of a standardized method of inducing this nerve injury. Various methods have been reported in the literature to deliver the crush injury, including various surgical instruments (Bridge et al., 1994; Kingery et al., 1994; Navarro and Kennedy, 1989) and compression devices (Chen et al., 1992; Oliveira et al., 2001; Radevik and Lundborg, 1977) with different crush durations. Therefore, a quantifiable method, in terms of pressure as well as duration of the compression, was used in order to standardize the crush damage and thus, avoid additional variations in functional and morphologic recovery.

Such a study might serve as a control for functional and structural recovery to apply in experiments facing the development of therapeutic methodologies in the rat sciatic nerve model for axonotmesis.

MATERIALS AND METHODS

Experimental Animals

The experiments in this study were performed on 19 Wistar adult male rats (Charles River, Barcelona, Spain) weighing approximately 275 g. Five more animals were used as controls. The animals were housed on sawdust, with five animals per makrolon cages (type 4). A piece of wire mesh (0.55 cm), measuring 35-cm-long and 22-cm-wide, was placed inside each cage at an angle of 45° to provide continuous physiotherapy. The animals had free access to food and water with a 12-h light/12-h dark cycle. To prevent autotomy after denervation a bitter spray (Specicare, Uldum, Denmark) was applied to the left foot once daily during the regenerative process. All procedures were performed with the approval of the Veterinary Authorities of Portugal in accordance with the European Communities Council Directive 86/609/EEC.

Surgical Procedure

The animals were anaesthetised with an intraperitoneal injection of a premixed solution containing ketamine (100 mg/kg) plus xylazine (5 mg/kg). After shaving and preparing the skin with 10% povidone iodine, the left sciatic nerve was exposed through the gluteal-splitting approach. In group A ($n = 17$), a non-serrated clamp, exerting a force of 54 N, was used for a period of 30 sec to create a 3-mm-long crush injury, 10 mm above the bifurcation, in order to get a good reproducibility of the axonotmetic lesion (Beer et al., 2001). The starting diameter of the sciatic nerve was about 1 mm; during the crush, the nerve flattens to a new diameter of 2 mm, giving a final pressure of $p = 9$ MPa. Group B ($n = 2$) underwent sciatic nerve transduction without repair. The nerves were kept moist with 37°C sterile saline solution throughout the surgical procedure. The muscle and skin were then closed with 4/0 resorbable sutures. The surgery was performed with the aid of an M-650 operating microscope (Leica, Wetzlar, Germany). The five un-crushed animals were used as controls (group C).

Functional Assessment of Reinnervation

Fifteen rats from Group A were evaluated for SFI, EPT, and WRL preoperatively (week 0), thereafter weekly until the end of the study (week 8). For analysis of biomechanical behavior, at week 0, and weeks 1, 4, and 8 postoperatively, the following parameters were measured during the stance phase of walking: the ankle kinematics, the toe out angle (TOA), and the gait-stance duration. Additionally, the MNCV and the gastrocnemius-soleus weight were calculated at the conclusion of

the study. Care was taken to minimize any stress that could interfere with the functional assessment.

Sciatic functional index. Animals were tested in a confined walkway measuring 42-cm-long and 8.2-cm-wide, with a dark shelter at the end. A white paper was placed on the floor of the rat walking corridor. The hind paws of the rats were pressed down onto a finger paint-soaked sponge, and they were then allowed to walk down the corridor leaving its hind footprints on the paper. Several measurements were taken from the footprints: (I) distance from the heel to the third toe, the print length (PL); (II) distance from the first to the fifth toe, the toe spread (TS); and (III) distance from the second to the fourth toe, the intermediary toe spread (ITS). All three measurements were taken from the experimental (E) and normal (N) sides. The SFI was calculated as described by Bain et al. (1989) according to the following equation:

$$\mathrm{SFI} = -38.3\left(\frac{\mathrm{EPL} - \mathrm{NPL}}{\mathrm{NPL}}\right) + 109.5\left(\frac{\mathrm{ETS} - \mathrm{NTS}}{\mathrm{NTS}}\right) + 13.3\left(\frac{\mathrm{EIT} - \mathrm{NIT}}{\mathrm{NIT}}\right) - 8.8 \quad (1)$$

The SFI oscillates around 0 for normal nerve function, and around −100 represents total dysfunction.

Extensor postural thrust. The motor performance was also examined by a functional test proposed by Thalhammer et al. (1995) as part of neurologic evaluation in the rat sciatic nerve model. The entire body of the rat, with the exception of the hind limbs, was wrapped in a surgical towel. EPT was elicited by supporting the animal by the thorax and lowering the afforded hind limb to the platform of a digital balance (digital scale with a range of about 0–500 g). As the animal was lowered, it extended its hind limb onto the surface of the balance (model TM 560; Gibertini, Milan, Italy). The force in grams applied to the digital platform balance was recorded, and the EPT of the contralateral, unaffected limb was recorded as well. The normal EPT (NEPT) and experimental EPT (EEPT) values were incorporated into a formula for calculating the percentage functional deficit, as decsribed later by Koka and Hadlock (2001):

$$\text{Percentage motor deficit} = (\mathrm{NEPT} - \mathrm{EEPT})/\mathrm{NEPT} \times 100 \quad (2)$$

Withdrawal reflex latency. Nociceptive function was examined using a modified unilateral hotplate test developed by Masters et al. (1993). The rat was wrapped in a surgical towel above its waist and then positioned to stand with the affected hind paw on a hot plate at 56°C (model 35-D; IITC Life Science Instruments, Woodland Hill, CA) and the other on a room temperature plate. The duration of stimulation necessary to induce a flexor reflex of the hind paw was measured with a stopwatch and termed WRL. Normal rats withdraw their paw from the plate within 4.3 sec or less (Hu et al., 1997). The affected limbs were tested three times, with an interval of 2 min between consecutive tests to prevent the sensitization phenomena, and then the three latencies were averaged. If no withdrawal occurred from the hot plate within 12 sec, the trial was terminated to avoid skin damage to the plantar surface of the foot, and the termination time was recorded.

Kinematic analysis. Computerized analysis of rat gait during the stance phase of walking included the study of the ankle kinematics, the TOA, and the gait stance duration. The walking track apparatus consisted of Perspex with a length of 120 cm, width of 12 cm, and height of 15 cm. In order to ensure locomotion in a straight direction, the width of the apparatus was adjusted to the size of the rats during the experiments, and a darkened cage was connected at the end of the corridor to attract them. A high-speed digital image camera (Dalsa CA-D1, Ontario, Canada) recorded the gait at 225 images per second and was positioned at the middle of the track, which was where the rats walked easily and spontaneously without acceleration or deceleration. The digital camera was connected to a PCI frame grabber (model R12; Bitflow Road Runner, Woburn, MA) where the images were stored and sent to the host computer.

To evaluate the ankle kinematics a recently developed two-segment biomechanical model was used (Varejão et al., 2002). The following four skin landmarks were used to describe ankle motion in the sagittal plane: the proximal point of the lower third of the tibia, lateral malleolus, calcaneus, and fifth metatarsal head. In order to identify the activity of the dorsiflexor and plantarflexor muscles of the rat ankle, the following formula was used:

$$\theta\ \text{Ankle} = \theta\ \text{foot} - \theta\ \text{leg} - 90^\circ \quad (3)$$

Neurologically, when there is an upward travel of the foot the θ ankle is positive, reflecting dorsiflexion; if the θ ankle is negative, it reflects an ankle's downward motion and is termed plantarflexion. For this kinematic analysis, the camera was positioned about 1 m away from the track to provide a direct lateral view of the animal during walking, and its magnification was calibrated so that it covered at 14-cm length of the track center. Four satisfactory walking trials per rat were obtained.

For kinematic analysis, only the walking trials in which the duration of the stance phase was between 150 and 400 msec were considered for statistical analysis, because this period of time is related to the range of normal walk-

ing velocity of the rat, 20–60 cm/sec (Hruska et al., 1979; Clarke and Parker, 1986). Temporal parameters were normalized to the total stance duration. Cubic-spline interpolation was applied to the original data about the angular position of the ankle to obtain 201 samples per stance phase, regardless of stance duration. This numerical treatment was performed with Matlab computational software (The MathWorks, Natick, MA). The normalized temporal parameters were averaged over all recorded trials. The data was expressed as means ± standard deviations.

To calculate the TOA and the gait-stance duration, the corridor's floor was monitored using the same equipment via a mirror placed at an angle of 45°, in order to get the plantar and side-view of the rat's hind paw (Westerga and Gramsbergen, 1990). The TOA was defined by the angle in degrees between the long axis of the foot (from the calcaneus to the tip of the third digit) and the line of progression. This functional index was evaluated when the foot remained flat on the floor, just before the swinging leg passes the stance leg (Varejão et al., 2003a). The gait-stance duration technique introduced by Walker et al. (1994a) was used to calculate the ratio of time of floor contact between the injured and uninjured hind paw. This ratio was calculated from paired consecutive steps and measured during spontaneously walking.

Motor nerve conduction velocity. At the end of the survival period, the MNCV studies were performed under general anesthesia, and were carried out with a Neuromatic 2000 M/C Neuro-Myograph (Dantec Elektronic Medicinsk Og Videnskabeligt Maleudstyr A/S, Skovlunde, Denmark). The sciatic nerve was percutaneously stimulated with supramaximal stimulus intensity through monopolar needle electrodes, proximal to the injury site at the level of the sciatic notch, and distal to the lesion at the level of the ankle. Square wave stimulus pulses of 500 μsec in duration were delivered at 1 Hz. Recorded signals were amplified with an alternating current-coupled preamplifier with filters at 1 Hz and 10 KHz. The latency of the evoked muscle action potentials were recorded from the intrinsic foot muscles with surface electrodes. Finally, the distance between the two sets of stimulating electrodes was measured on the skin with a ruler to the nearest 1 mm, and the conduction velocity was calculated. Both experimental (left) and normal (right) nerves were measured. MNCV data were calculated as percentages of functional deficit for the contralateral nerve of the same rat.

Gastrocnemius and soleus muscle weight. The gastrocnemius and soleus muscle groups of the experimental and unoperated sides of each animal were dissected free from its origin and insertion and weighed immediately while still wet at time of euthanasia. Gastrocnemius and soleus muscle weight data were calculated as percentages of those for the contralateral unaffected limb of the same rat to correct for individual differences.

Morphological Analysis

At 2 weeks after the beginning of the experiments, in order to confirm the Wallerian degeneration, two animals from group A (crush lesion) and both animals from group B (nerve transection without repair) were euthanasized and a 10-mm-long sample of the left sciatic nerve segment distal to the lesion was removed, fixed, and prepared for light and electron microscopic examination. All other rats from group A ($n = 15$) were euthanasized 8 weeks after the crush lesion. From seven of these rats, a 10-mm-long sample of the left sciatic nerve segment distal to the crush was removed, fixed, and prepared for light and electron microscopy examination and histomorphometry of myelinated nerve fibers. From the 5 uncrushed animals of group C, the left normal sciatic nerves were taken as controls.

The crushed sciatic nerves were immersed immediately in a drop of fixation solution, containing 2.5% purified glutaraldehyde and 0.5% saccharose in 0.1M Sorensen phosphate buffer (pH 7.4, 4°C). A 10-mm-long segment of the nerve distal to the crush was excised and immersed immediately in a drop of fixation solution keeping the specimen well distended and oriented for about 5 min. Specimens were then immersed in the fixation solution for 6–8 h. Specimens were washed in a solution containing 1.5% saccharose in 0.1M Sorensen phosphate buffer (pH 7.4) for 6–12 h. The nerves were then post-fixed in 1.5% osmium tetroxide, dehydrated and embedded in Glauerts' embedding mixture of resins consisting in equal parts of Araldite M and the Araldite Härter, HY 964 (Merck, Darmstad, Germany), to which was added 2% of the accelerator 964, DY 064 (Merck, Darmstad, Germany). The plasticizer dibutyl phthalate was added in a quantity of 0.5%.

Light microscopy. Series of 2-μm-thick semi-thin transverse sections were cut using an Ultratome-III ultramicrotome (LKB, Bromma, Sweden) and stained by Toluidine blue for 2–3 min for high-resolution light microscopy examination.

Transmission electron microscopy. Ultra-thin sections were cut immediately after the series of semi-thin section by means of the same ultramicrotome and stained with saturated aqueous solution of uranyl acetate and lead citrate. The sections were then analyzed using a JEM-1010 transmission electron microscope (JEOL, Tokyo,

Japan) equipped with a Mega-View-III digital camera and a Soft-Imaging-System (SIS, Münster, Germany) for the computerized acquisition of the images.

Histomorphometry. Quantitative morphology of myelinated nerve fibers was carried out on the five un-crushed control nerves (group C, codes: N1-N5) and on seven crushed nerves sampled 8 weeks after the lesion (group B, codes: A9-A15). In each nerve, histomorphometry was conducted using a Videoplan Image Processing System (Carl Zeiss, Jena, Germany), composed of a camera and a Digicad graphic tablet connected to a Laborlux-S light microscope (Leitz, Wetzlar, Germany). The graphic tablet was connected to an IBM 286 PC computer. This system reproduced microscopic images (obtained through a ×100 oil-immersion Leitz objective) on the monitor at a final magnification of ×3,720. This permitted accurate recognition, counting and measurement of myelinated nerve fibers. One semi-thin section from each series was randomly selected and used for the morpho-quantitative analysis. The total cross-sectional area of each nerve profile was measured. The sampling fields were then selected inside the nerve profile as previously described (Geuna et al., 2000, 2001) and myelinated nerve fiber profiles were counted and measured. To cope with the "edge effect" we employed a two-dimensional disector procedure which is based on sampling the "tops" of fibers (Geuna et al., 2000, 2004). Once the number of fibers was counted in each sampling field, their density was calculated as the number per mm^2 (N/mm^2). Total fiber number (N) were then estimated by multiplying the mean fiber density by the total cross-sectional area of the whole nerve cross section. Fiber and axon area were measured and the circle-fitting diameter of fiber (D) and axon (d) were calculated. Then from these data, we have also calculated myelin thickness [(D − d)/2], myelin thickness/axon diameter ratio [(D − d)/2d], and fiber/axon diameter ratio (D/d).

Analysis of the sampling scheme was peformed by calculating the coefficient of error (CE) that is a measure of the precision of the quantitative estimates.

As regards quantitative estimates on fiber number, the following formula for computing the *CE(n)* was used (according to Schmitz, 1998):

$$CE(n) = \frac{1}{\sqrt{\Sigma Q'}} \quad (4)$$

where $\Sigma Q'$ is number of counted fibers in all disectors.

For size estimates, the coefficient of error of the mean size was estimated as (according to Geuna et al., 2001):

$$CE(z) = \frac{SEM}{Mean} \quad (5)$$

where SEM = standard deviation of the mean.

During the pilot study phase, the sampling scheme was designed in order to keep the CE below 0.10, a value that allows obtaining a sufficient estimate precision for neuromorphological studies (Pakkenberg and Gundersen, 1997).

Statistics

For functional data, the overall effects of the crush lesion were assessed with one-way repeated measures analysis of variance (RM-ANOVA) test applied on the values from all the time-point assessments. When the presence of significant changes was observed, post-hoc multiple pairwise comparisons were carried out using the Student-Neuman-Keuls (SNK) test. For histomorphometry, statistical comparisons of quantitative data were subjected to one-way ANOVA test. Statistical significance was established as $p < 0.05$. All statistical tests were performed using the software "Statistica per Discipline Bio-Mediche" (McGraw-Hill, Milan, Italy).

RESULTS

Immediately after the acute compression injury, the crushed areas of all sciatic nerves were flattened, but nerve continuity was not interrupted grossly. Complete flaccid paralysis of the operative foot was observed following crush injury. All rats survived, with no wound infection, and automutilation was restricted to the absence of nails in the most lateral digits of 3 animals.

Functional Assessment of Reinnervation

Sciatic functional index (Fig. 1A). Reproducible walking tracks could be measured from all rats. In each walking track three footprints were analysed by a single observer, and the average of the measurements was used in SFI calculations. After week 1, SFI had decreased to -97.5 ± 8.2 and then it began to recover progressively until the end of the experiment. The RM-ANOVA test discerned overall statistically significant differences in the SFI between time-point assessments [$F(14,120) = 295.1$, $p < 0.05$]. Post-hoc multiple comparisons by the SNK test showed that the numerical differences detected between all pairs of time-point assessments were statistically significant ($p < 0.05$), except for the comparison between SFI assessments made at week 0, week 7, and week 8, indicating that function gradually returned to normal in 7 weeks.

Extensor postural thrust (Fig. 1B). The RM-ANOVA test found overall statistically significant differences in the EPT between time-point assessments [$F(14,120) =$

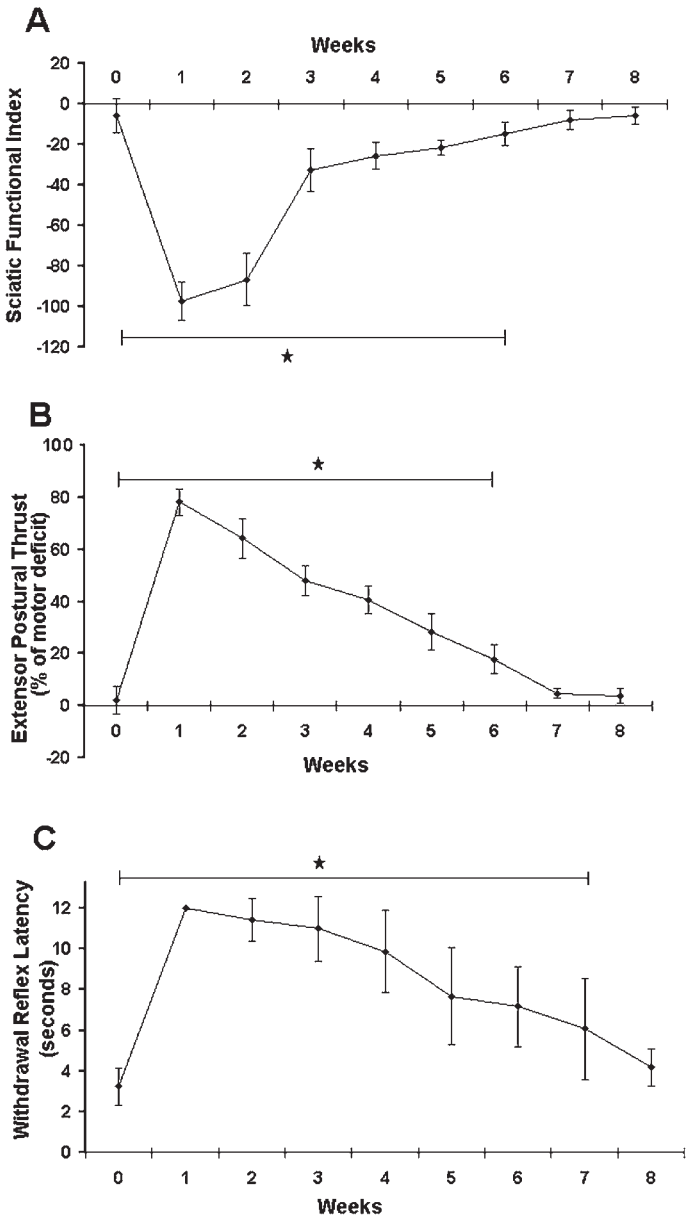

FIG. 1. Time course of functional recovery following crush injury. (**A**) Sciatic functional index. (**B**) Extensor postural thrust. (**C**) Withdrawal reflex latency. All values are given as means ± standard deviations; *$p < 0.05$.

371.4, $p < 0.05$]. Post-hoc multiple comparisons by the SNK test showed that, similar to the previous parameter, the numerical differences detected between all pairs of time-point assessments were statistically significant ($p < 0.05$) except for the comparison between assessments made at week 0, week 7 and week 8 indicating that, after the great impairment observed at week 1, EPT values gradually returned to preinjury levels in 7 weeks.

Withdrawal reflex latency (Fig. 1C). The RM-ANOVA test found overall statistically significant differences in the WRL between time-point assessments [$F(14,120) = 212.4$, $p < 0.05$]. Post-hoc multiple comparisons by the SNK test showed that the loss of nociceptive function observed at week 1 was statistically significant ($p < 0.05$) and remained relatively stable for the next 3 weeks ($p < 0.05$). The first signs of nociceptive withdrawal reflex could be observed at week 4 and, after then, WRL pro-

gressively decreased, returning to values not significantly ($p > 0.05$) different from preoperative values at the end of the study (week 8).

Ankle kinematics (Fig. 2 and Table 1). To characterize two-dimensional motion of the foot and ankle, a total of 240 walking trials from 15 rats were obtained. The stance phase duration averaged 279.1 ± 61.2 msec, 257.6 ± 65.4 msec, 267.4 ± 75.1 msec, and 273.9 ± 65.1 msec for the left hind limb preoperatively, and postoperatively at weeks 1, 4, and 8, respectively. In order to describe the angular movement of the ankle, according to the foot placement of the hind limbs, we used the previously published terminology (Varejão et al., 2002). **Initial contact (IC):** The RM-ANOVA test found overall statistically significant differences in the initial foot contact between time-point assessments [$F(14,45) = 69.2$, $p < 0.05$]. Post-hoc multiple comparisons by the SNK test showed that the numerical differences detected between all pairs of time-point assessments were statistically significant ($p < 0.05$) except for the comparison between IC assessments made at week 4 and week 8. These results indicated that, while during normal walking in rats the initial food contact is made with the digits and the ankle is plantarflexed, 1 week after injury this foot event was processed in dorsiflexion with an abrupt fall of the plantar surface of the paw. After 4 weeks, the ankle mobility changed from dorsiflexion to plantarflexion with an angle at IC that was significantly ($p < 0.05$) higher than baseline. This effect of the crush injury was still present after 8 weeks ($p < 0.05$). **Opposite toe-off (OT):** the RM-ANOVA test found overall statistically significant differences in the opposite toe-off event [$F(14,45) = 99.6$, $p < 0.05$]. Post-hoc multiple comparisons by the SNK test showed that the numerical differences detected between all pairs of time-point assessments were statistically significant ($p < 0.05$) except for the comparison between OT assessments made at week 0 and week 4 indicating that both the increase in the dorsiflexion observed at week 1, with the tibia moving in an exaggerated way forward over the foot, and the plantarflexion observed at week 8 were significant. **Heel-rise (HR):** In normal rats the HR is the time when the proximal pads begin to lift, but following sciatic denervation we had to

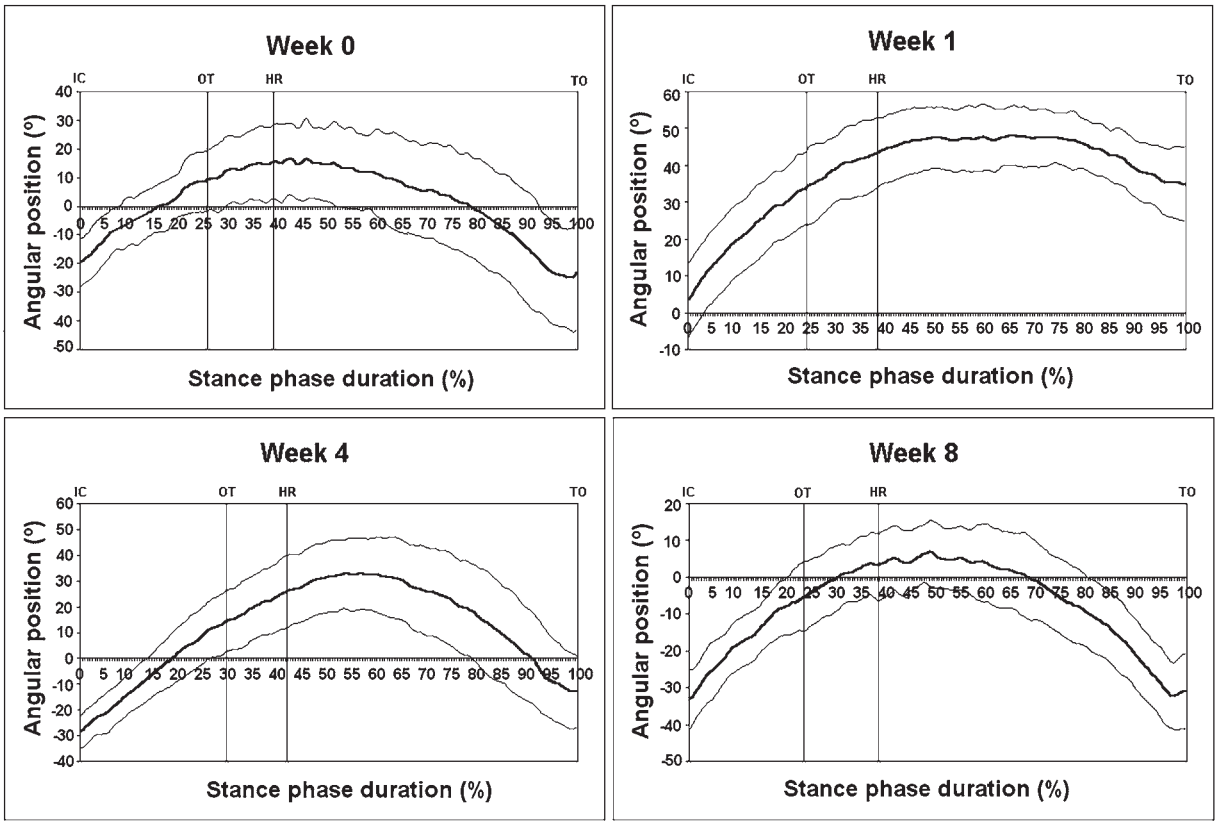

FIG. 2. Kinematic plots of the ankle in the sagittal plane as it moves through the stance phase, during the crush injury study. Standard deviation is plotted on either side of the mean. IC, initial contact; OT, opposite toe-off; HR, heel-rise; TO, toe-off.

Table 1. Ankle Joint Angles

Ankle motion	*Week 0*	*Week 1*	*Week 4*	*Week 8*
Initial contact	−19.5 ± 8.3°	3.6 ± 10.2°	−28.5 ± 6.4°	−33.1 ± 8.0°
Opposite toe-off	8.7 ± 10.6°	34.2 ± 10.4°	13.9 ± 11.9°	−4.9 ± 9.4°
Heel-rise	15.2 ± 12.8°	43.9 ± 9.5°	25.4 ± 14.0°	3.4 ± 8.6°
Toe-off	−23.2 ± 19.7°	34.8 ± 10.1°	−12.7 ± 14.0°	−31.1 ± 10.2°

Values represent means and standard deviations; positive values indicate ankle dorsiflexion, and negative values indicate ankle plantarflexion.

define it as the moment when the swinging leg passes the stance phase. The RM-ANOVA test found overall statistically significant differences in the heel-rise event [$F(14,45) = 111.5$, $p < 0.05$]. Post-hoc multiple comparisons by the SNK test showed that the numerical differences detected between all pairs of time-point assessments were statistically significant ($p < 0.05$), indicating that both the increase in the dorsiflexion of the ankle value observed at week 1 and week 4 and the reduction in dorsiflexion from baseline detectable at week 8, were significant. At the end of the experiment (week 8), accordingly to formula 3, the foot was approximately at right angles to the leg ($p < 0.0001$). **Toe-off (TO):** In normal animals at TO the foot-ankle was plantarflexed. The RM-ANOVA test found overall statistically significant differences [$F(14,45) = 128.3$, $p < 0.05$]. Post-hoc multiple comparisons by the SNK test showed that only the TO differences detected between week 0 and week 1, week 1 and week 4, and week 1 and week 8 were statistically significant ($p < 0.05$) indicating that the denervation at week 1 changed the ankle position towards a high value of dorsiflexion, while all the plantar surface of the foot remained in contact with the ground. At week 4 and 8 the TO was already made with the ankle in plantarflexion and the numerical differences observed between these two time-point assessments and preinjury assessments were not statistically significant ($p > 0.05$).

Toe-out angle (Fig. 3A). The RM-ANOVA test found overall statistically significant differences [$F(14,45) = 47.3$, $p < 0.05$]. Post-hoc multiple comparisons by the SNK test showed that the large increase in TOA values detectable at week 1 and week 4 post-crush was statistically significant ($p < 0.05$). At the latter time point, the animals had regained normal TOA values ($p > 0.05$).

Gait-stance duration (Fig. 3B). The RM-ANOVA test discerned overall statistically significant differences in the gait-stance duration [$F(14,45) = 27.5$, $p < 0.05$]. Post-hoc multiple comparisons by the SNK test showed that the numerical differences detected between all pairs of time-point assessments were statistically significant ($p < 0.05$) except for the comparison between gait-stance duration assessments made at week 0 and week 8 indicating that, after crush injury, the ratio of injured/uninjured hind limb gait-stance duration decreased significantly at week 1 and week 4, whilst at week 8, the animals had recovered to normal levels.

Motor nerve conduction velocity. The MNCV recorded from the normal limbs averaged 45.6 ± 3.2 m/sec. At week 8 the functional deficit in MNCV was 43.1 ± 3.1%.

Gastrocnemius and soleus muscle weight. Gastrocnemius and soleus muscle groups on the operated sides demonstrated gross atrophy when compared to the contralateral normal limbs. Eight weeks after surgery, the functional deficit predicted by the gastrocnemius-soleus weight was 25.2 ± 5.6%.

Morphological Analysis

Light microscopy. Figure 4 shows a light micrograph of the nerve segment 5-mm distal to the crush site withdrawn two weeks after injury (A) comparing it to what happens in a nerve segment distal to an un-repaired complete transection (B). The light microscope morphology is very similar and points to the presence of an active process of Wallerian degeneration in both conditions. This observation provided the evidence that the crush lesion did really interrupt the continuity of axons inducing the degeneration of their distal stump.

Figure 5 shows a comparison between a normal rat sciatic nerve and a regenerated nerve withdrawn 8 weeks after the crush injury. Regenerated nerves showed the presence of myelinated fibers with smaller caliber and a thinner myelin sheath in comparison to normal nerve. Microfasciculation, typical of regenerated nerve fibers is also clearly detectable.

Transmission electron microscopy. Ultrastructural analysis confirmed the observations made by light microscopy. The comparison of the electron microscope pictures taken at week-2 post-crush (Fig. 6) and at week-

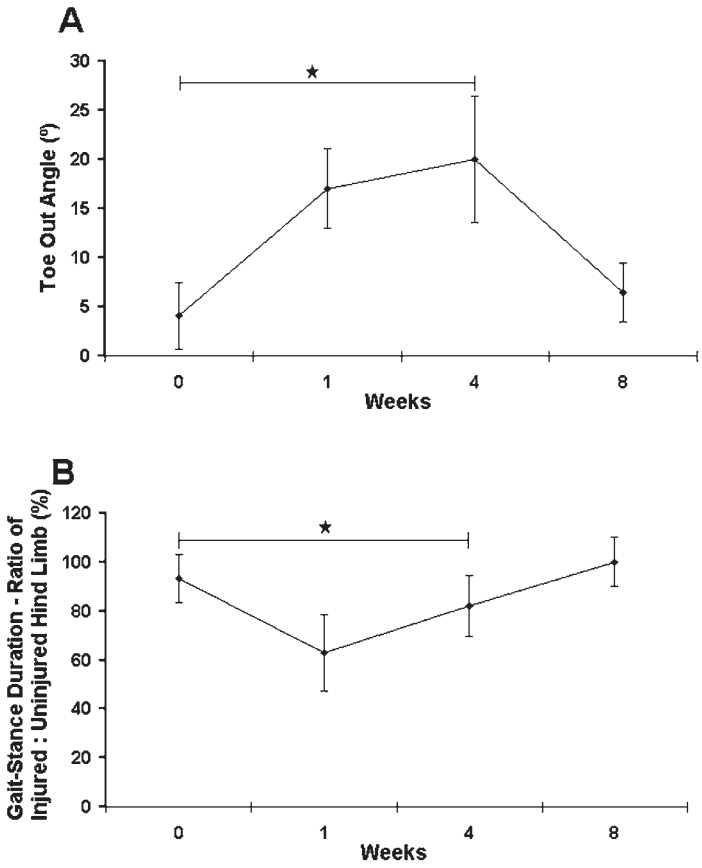

FIG. 3. Time course of functional recovery following crush injury. (**A**) Toe out angle. (**B**) Gait-stance duration. All values are given as means ± standard deviations. $^{\star}p < 0.05$.

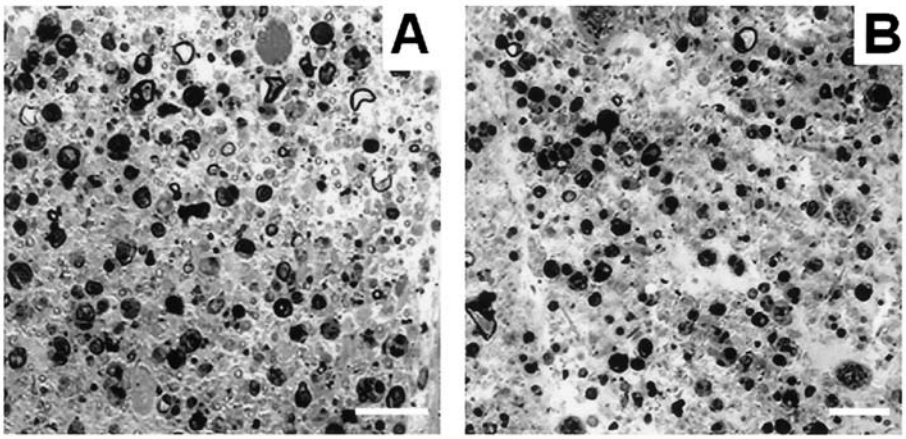

FIG. 4. Light micrographs of a nerve segment 5-mm distal to the crush site withdrawn 2 weeks after injury (**A**) and of a nerve segment distal to an un-repaired complete transection (**B**). At light microscopy, the two pictures look very similar, showing the typical features of Wallerian degeneration. Bar = 20 μm.

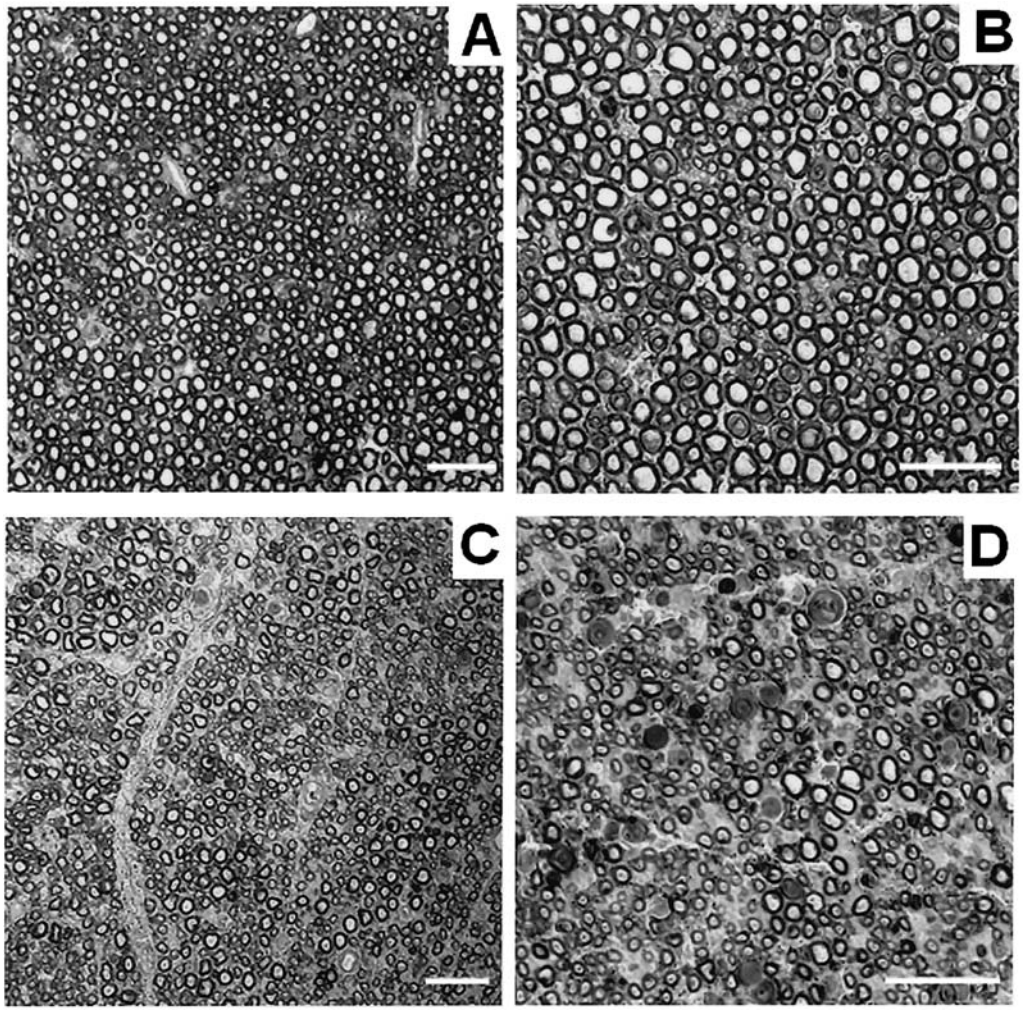

FIG. 5. Light micrographs of normal sciatic nerve (**A,B**) and regenerated sciatic nerve trunks distal to the crush, 8 weeks after injury, where a good regeneration pattern, with the typical microfasciculation, can be detected (**C,D**). Bar = 20 μm.

2 post complete nerve resection (Fig. 7) add important information to the observations made by light microscopy. While in the latter nerve samples all the images show pictures typical of Wallerian degeneration (Fig. 7), in post-crush nerves clear pictures of nerve fiber regeneration can be detected, mingled with the pictures showing the Wallerian degeneration that transected nerve fibers are undergoing. In fact, many small nerve fibers with a healthy, though still thin, myelin sheath are detectable only in crushed nerves (Fig. 6A,B) and not in transected nerves. These can thus be interpreted as the regenerated nerve fibers that already begun the myelination process. In addition, many bundles of "healthy" unmyelinated nerve fibers can be also found in crushed nerve (Fig. 6C,D) that can be interpreted as either regenerated unmyelinated fibers or regenerated nerve fibers that still had to begin the myelination process.

At week 8 post-crush, an advanced stage of regeneration can be detected (Fig. 8). Only few degeneration features (arrows) can be still observed among the many regenerated fibers, both myelinated (Fig. 8A,B) and unmyelinated (Fig. 8D). The presence of fibers that are still in a very early phase of myelinization (Fig. 8C,E) demonstrates that, at week-8 post-crush injury, the process of maturation of regenerated nerve fibers, though very fast in these experimental conditions, is still not complete.

Histomorphometry. Results of the morphometrical analysis of normal (uncrushed) sciatic nerves and regenerated sciatic nerves (8 weeks after crush) are reported in Tables 2 and 3. The increase in the mean density and

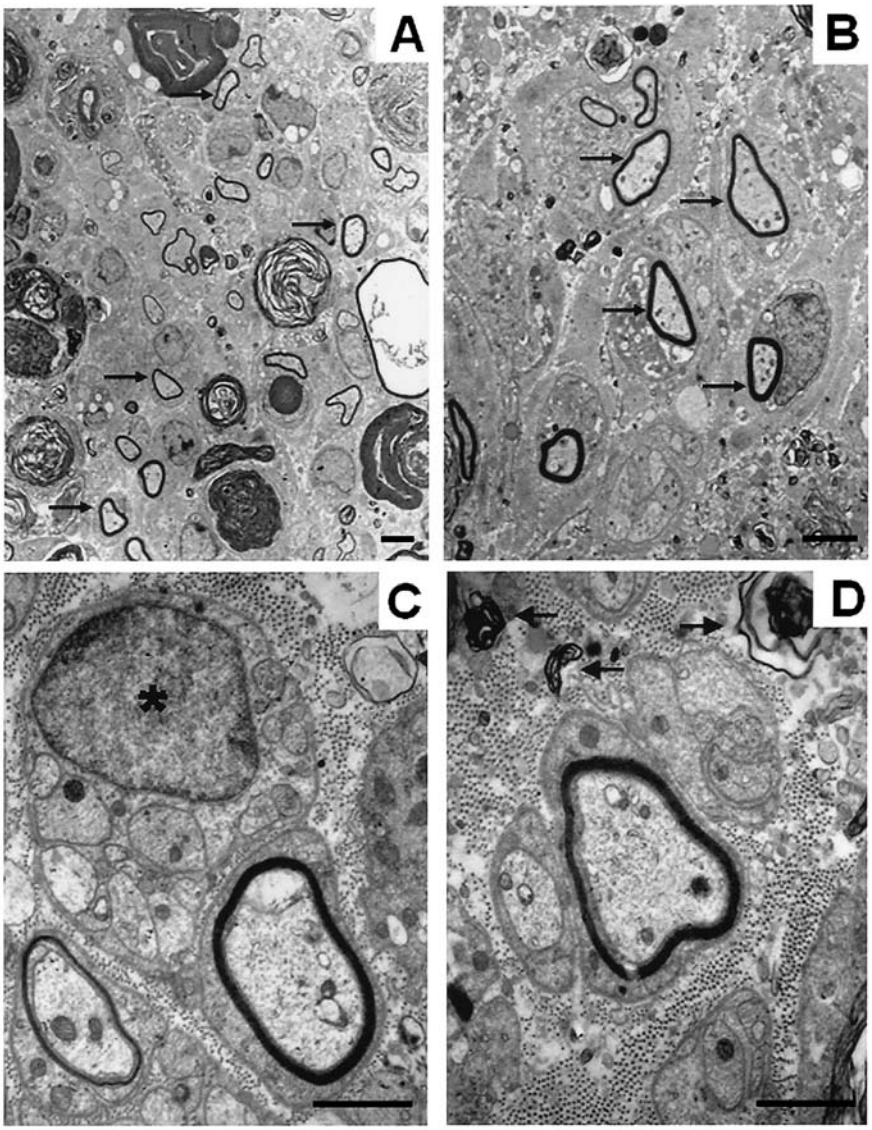

FIG. 6. Regenerated sciatic nerve trunks distal to the crush (2 weeks after lesion) showing a nascent process of nerve fiber regeneration with many small nerve fibers (arrows) in a background of Wallerian degeneration (**A,B**). Schwann cells (asterisk) ensheathing small unmyelinated axons can be frequently detected (**C**). Myelin sheaths are very thin (**D**). The arrows in (D) indicate masses of myelin debris. Bar = 2 μm (A,B), 1 μm (C,D).

total number of myelinated fibers in regenerated nerves, in comparison to normal values, was statistically significant ($p < 0.01$). The same was true also for the decrease in mean fiber diameter, axon diameter and myelin thickness observed in regenerated nerves ($p < 0.01$). By contrast, for the other two parameters (myelin thickness/axon diameter ratio and fiber/axon diameter ratio) the numerical differences observed between the nerves that received crush injury and controls were not statistically significant ($p > 0.1$).

Figure 9 shows the histograms of the size value distributions of nerve fiber diameters in normal sciatic nerves (Fig. 9A) and in regenerated nerves 8 weeks after crush injury (Fig. 9B). The typical bimodel distribution of myelinated nerve fiber diameters can be observed in normal sciatic nerves only, whereas in regenerated nerves there is a clear trend towards smaller sizes, with a prevalence of nerve fibers with diameters <5 μm.

DISCUSSION

Axonotmesis, or second-degree Sunderland injury, designates a breakdown of the axon and distal Wallerian

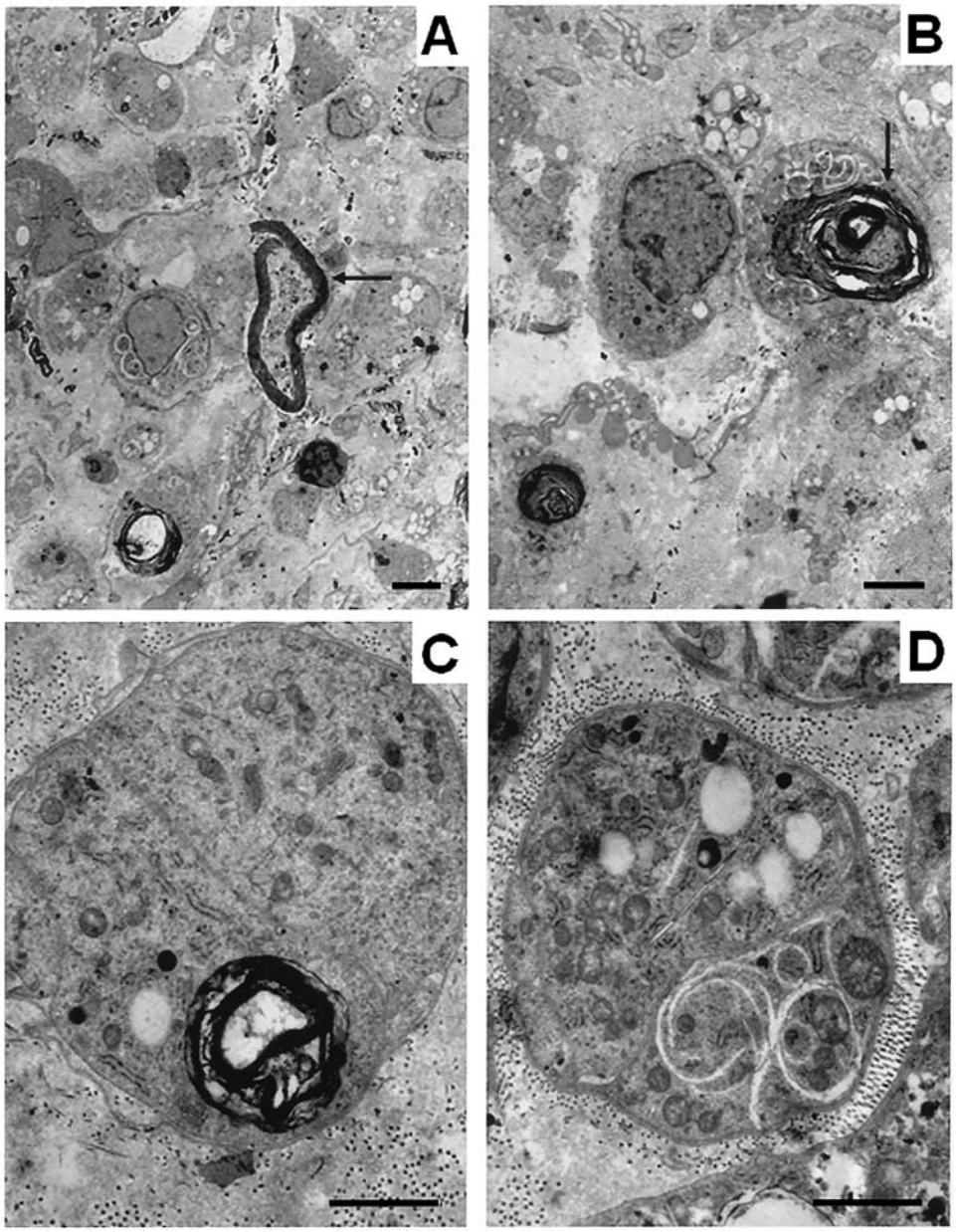

FIG. 7. Sciatic nerve trunks distal to a complete transection not followed by nerve fiber regeneration from the proximal stump (2 weeks after lesion). Typical pictures of Wallerian degeneration can be detected with some isolated myelinated nerve fiber still recognizable within the degeneration framework (**A**, arrow) while most fibers are completely degenerated and are being phagocytosed by the macrophages (**B**, arrow). The ultrastructural appearance of macrophage-like cells is shown in (**C–D**), with myelin debris inside the cytoplasm. Bar = 2 μm (A,B), 1 μm (C,D).

degeneration but with preservation of the continuity of the endoneurial sheath. After this type of injury, spontaneous regeneration through the distal nerve stump with good functional return can be expected (Seddon, 1943; Sunderland, 1951, 1990). As the restored pattern of innervation is identical to the original, the study of this nerve lesion provides a good model for establishing the ontogeny of functional nerve recovery.

Since functional testing of the rat hind paw after sciatic nerve injury depends on the integrity of the denervated digits and on ankle and digits mobility, two important strategies were adopted in our model. First, for prevention of autotomy a deterrent substance was applied to their left foot (Kerns et al., 1991; Sporel-Ozakat et al., 1991). Second, the wire-mesh as a post-operative assistive device (Strasberg et al., 1996) was used in order to

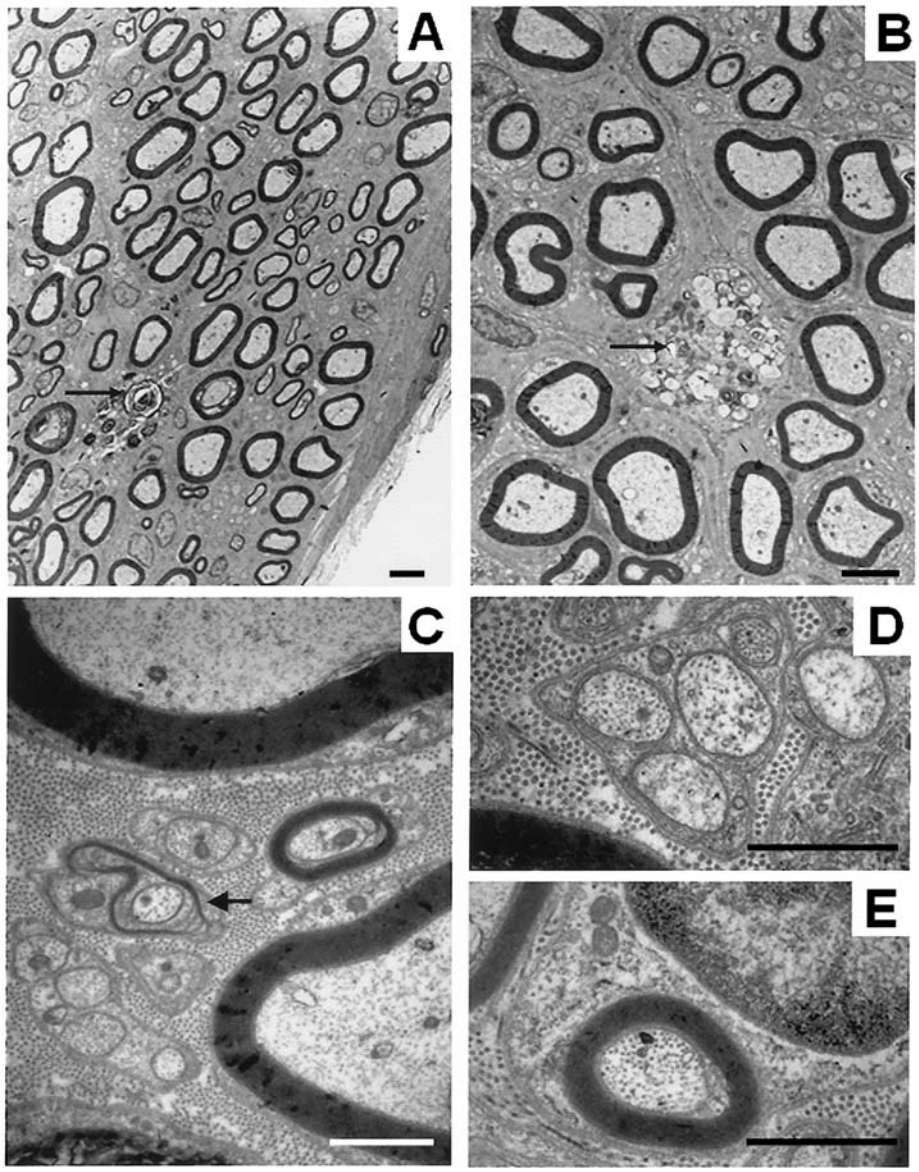

FIG. 8. Regenerated sciatic nerve trunks distal to the crush (8 weeks after lesion). The regeneration process is already in an advanced stage and only few degeneration features (arrows) remain among many regenerated fibers (**A,B**). Although the regeneration process is at an advanced stage, very small myelinating axons can still be detected mingled with many unmyelinated nerve fibers (**C–E**; the arrowhead in C points to a fiber in a very early myelinating stage). Bars = 2 μm (A,B), 1 μm (C), 0.5 μm (D,E).

preserve the ankle range of motion and prevent toe contractures.

Since its introduction by de Medinaceli et al. (1982), the SFI has become the mainstay of the functional arsenal to assess the global functional recovery after sciatic nerve injury (Varejão et al., 2001a,b). After a pressure of 9 MPa was exerted to the nerve, a complete functional deficit was evident in all animals, subsequently the SFI increased and normal values were achieved at week 7. These results are in line with the findings of several authors whose studies have also shown normal walking patterns only after the first month of postcrush (Carlton and Goldberg, 1986; Chen et al., 1992; Gudemez et al., 2002; Oliveira et al., 2001). In contrast to these experiments, others reported a full recovery already during the third and fourth weeks (Bridge et al., 1994; Hare et al., 1992; Walker et al., 1994b). The difference in the rate of motor functional recovery may relate to the pathophysio-

Table 2. Histomorphometrical Assessment of Normal Sciatic Nerves

Code	*N/mm², density*	*N, number*	*D, fiber diameter*	*d, axon diameter*	*(D-d)/2, myelin thickness*	*(D-d)/2d*	*D/d*
N1	10,679	8,319	7.06	4.87	1.11	0.23	1.45
N2	12,060	8,546	7.19	4.87	1.16	0.25	1.48
N3	11,518	8,130	7.13	4.75	1.19	0.26	1.50
N4	10,569	8,198	7.24	5.06	1.09	0.22	1.43
N5	12,383	7,957	7.45	5.30	1.09	0.20	1.42
Mean ± SD	11,442 ± 809	8,230 ± 220	7.21 ± 0.15	4.97 ± 0.22	1.13 ± 0.04	0.23 ± 0.02	1.46 ± 0.03

logic response of peripheral nerves to the magnitude of different crushing loads (Lundborg and Dahlin, 1992; Rempel et al., 1999).

The EPT proposed by Thalhamer et al. (1995) to evaluate the hind limb motor function in rats, is now a well established technique in peripheral nerve research (Hadlock et al., 2001; Hu et al., 1997). This method measures the force in grams generated by the foot against the surface of the balance, as a result of the extension of the gastrocnemius-soleus muscles, similar to the peak vertical force parameter obtained by the study of the ground reaction forces (Clarke et al., 2001; Howard et al., 2000). On the seventh week after crush, it was no longer possible to detect deficits through the analysis of this functional parameter. The speed of functional recovery observed with this method was consistent with the values obtained by the SFI, based on measurement of the footprints. This is in agreement with recent studies, where the results of time recovery through EPT and SFI assessments were very similar (Hadlock et al., 1999; Koka and Hadlock, 2001).

The first signs of withdrawal response evoked by thermal noxious stimulation were observed only after the third week. Hadlock et al. (1999), using the hot plate test, also found a slower recovery pattern of the sensory function compared with motor recovery profile. Interestingly, when the nerve is transected and the regenerating axons must bridge a gap, sensory neurons exhibit a faster regenerative pattern than motor neurons (Madorsky et al., 1998). In a crush injury study, Navarro et al. (1994) found an earlier appearance of nociceptive function when compared to motor function, which was evaluated by pricking with a needle on the plantar aspect of the medial side of the paw. However, in the specified anatomic evaluated area, saphenous nerve collateral sprouting has been reported to account for sensory recovery; therefore, the rate of return of nociception was probably artificially accelerated (Devor et al., 1979; Kingery and Vallin, 1989). When using the hot plate test it is important not to press the paw onto the heat source, in order to prevent the additional recruitment of mechanoreceptors (Kerns et al., 1991).

Our high-speed camera system used to track the changing positions and orientations of the foot and leg segments provided a quantification of the biomechanical behavior of the plantar flexors dysfunction. The normal rat ankle joint has a consistently recognizable pattern during the stance phase: a small plantar flexor movement followed by a dorsiflexor activity and before the foot leaves the ground, the ankle plantar flexes again. To attain this

Table 3. Histomorphometrical Assessment of Regenerated Sciatic Nerves (8 Weeks after the Crush Lesion)

Code	*N/mm², density*	*N, number*	*D, fiber diameter*	*d, axon diameter*	*(D-d)/2, myelin thickness*	*(D-d)/2d*	*D/d*
A9	21,800	10,021	4.86	3.53	0.73	0.24	1.48
A10	22,256	9,250	5.10	3.71	0.79	0.22	1.44
A11	21,980	11,233	4.29	3.01	0.78	0.29	1.59
A12	24,312	11,088	4.16	3.02	0.67	0.27	1.55
A13	19,536	9,462	4.45	3.47	0.69	0.22	1.43
A14	25,258	9,699	4.23	3.05	0.79	0.28	1.56
A15	28,741	11,272	4.10	3.17	0.63	0.22	1.43
Mean ± SD	23,412 ± 2,989	10,289 ± 883	4.46 ± 0.38	3.28 ± 0.28	0.73 ± 0.06	0.25 ± 0.03	1.50 ± 0.06

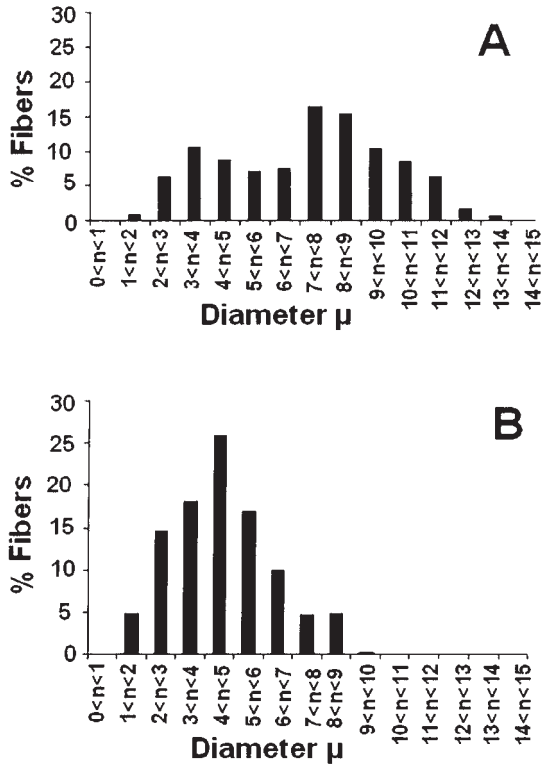

FIG. 9. Size distributions of nerve fiber diameters in normal nerves (**A**) and in regenerated nerves 8 weeks after crush injury (**B**). Nerve diameters have been grouped in classes of 1 μm, and the values are represented in percentage of fibers.

ankle angle pattern motion, the gastrocnemius-soleus muscles function either to provide resistance to dorsiflexion or to cause active plantar flexion (Varejão et al., 2002). After sciatic nerve crush injury the role of the calf muscles in controlling the sagittal plane of ankle motion is seriously affected, as recently reported (Varejão et al., 2003b). At week 1, the collapse of the tibia over the foot, and the inadequate propulsion at the end of the stance phase were depicted as a persistent dorsiflexion. At the end of the experiment, the angle values of the foot events at IC, OT, and HR were still statistically different from the preinjury levels and the range of the arcs of ankle motion seemed to be the result of an exaggerated activity of the plantarflexor muscles. We were unable to identify the cause for such hyperexcitability, but it might result from a central somatosensory topographic reorganization and an enlargement of the recepive fields (Doetsch et al., 1996; Churchill et al., 1998; Dupont et al., 2001; Langlet et al., 2001). In the Barbay et al. (2002) study, it was demonstrated that, between 2 and 4 months after the crush injury, the somatosensory cortex did not appreciably compensate for reinnervation errors. As early as 7 days following a peripheral nerve injury, the amount of cortex controlling its target muscles is modified in adult rats (Sanes et al., 1990). Moreover, distal organ reinnervation does not guarantee the restitution of normal spinal cord reflex function, as H reflex is facilitated after peripheral nerve injury (Valero-Cabré and Navarro, 2001). Another possible explanation for this hyperexcitability could be that the change in distribution of various fiber types in the calf muscles, the so-called fiber type-grouping of type I fibers and an increase in type II fibers, could affect the motor endplates after sciatic nerve lesion (IJkema-Paasen et al., 2001). The present study is the first to use the sagittal and transversal planes to get motion data in order to quantify the foot and ankle functional recovery in the rat, following damage to the peripheral nervous system. Despite the fact that most of ankle motion occurs in the sagittal plane in normal rats, after sciatic nerve injury the animals typically ambulate with an external rotation of the foot (Varejão et al., 2003a). Therefore, we used the transverse plane to provide data of foot malrotation using the TOA index. On the fourth week, the improvement in the sagittal plane of ankle motion was associated with a huge increase in the numerical value of TOA. This suggests that a finer control of the ankle joint trajectory may result from a compensation achieved mainly by an increment in the TOA (Carrier et al., 1997). With the reduction in the lever arm for the gastrocnemius-soleus muscles group, the forward propulsion is seriously affected (Leardini and O'Connor, 2002). The recovery of the TOA paralleled the time recovery of the gait-stance duration, with normal values at the end of the experiment.

The ankle kinematics reflects a coordinated recruitment of dorsiflexor and plantarflexor motor units which is not possible to investigate through the foot print analysis. We therefore believe that the accuracy of computerized analysis of rat gait is a good reason for its more general use in the future though, undoubtedly, the traditional methods of evaluation also have their place in peripheral nerve investigation, as they are noninvasive, easy to use, and of low cost.

The recordings of MNCV obtained for the normal rat sciatic nerves agreed well with previously published values (Carrington et al., 1991; Pu et al., 1999) and have standard deviations of less than 10% of the means, suggesting good testing conditions (Wells et al., 1997). At 8 weeks after a crush lesion, Van Meeteren et al. (1997) also found a functional deficit of about 40% in the MNCV. De Koning and Gispen (1987) reported a similar MNCV deficit after 8 weeks and a 30% deficit after 6 months. Additionally, in a long-term study after a crush lesion, it was reported that a fully normal MNCV is never regained by regenerated nerve fibers (Cragg and Thomas, 1964). It should be mentioned that MNCV studies de-

pend heavily on fiber diameter and degree of myelination, therefore it may not measure total nerve function, but it does measure the fastest fibers (Dorfman, 1990).

The gastrocnemius and soleus muscle weight provides indirect evidence of nerve regeneration and has been extensively used in functional recovery studies; however, its validity has been questioned by several investigators. As noted by Kanaya et al. (1992, 1996), it is important to consider that muscle weight can include nonfunctioning adipose tissue and fibrosis.

From a morphological point of view, a major criticism that can be made of the nerve crush model is related to the possibility that not all nerve fibers are structurally damaged by the crush lesion: that is, some nerve fibers might undergo only a temporary functional impairment (type I lesion according to Sunderland) and the following functional recovery could thus not be due to a true regeneration of the severed axons. The use of a non-standardized clamping procedure increases this problem.

Light and electron microscope observations obtained on nerves sampled at week 2 after the employment of the standardised crush procedure used in this study, showed that true Wallerian degeneration occurred in the nerve segments distal to the crush site. Mingled with many degenerating nerve fibers, electron microscope analysis showed the presence of abundant un-myelinated and thin myelinated axons, not detectable by light microscopy, which represent regenerating nerve fibers. Therefore, it can be concluded that the fibers that can be observed (and measured) at later post-operative times (8 weeks) were truly regenerated fibers and the information that can be derived from them can be directly related to a true regeneration process.

Qualitative morphological observations carried out at week-8 post-operatively, detected that regenerated myelinated fibers were smaller and showed a thinner myelin sheath in comparison to normal nerves. Microfasciculation, typical of regenerated nerve fibers, was also evident. Quantitative morphology provided us with more information on the regeneration process. In fact, while significant differences regarding density, number, size and myelin thickness of nerve fibers was detectable in regenerated nerves in comparison to controls, two morphometrical parameters (namely, myelin thickness/axon diameter ratio and fiber/axon diameter ratio) did not show significant differences from the controls. These results are in line with the observations of Kanaya et al. (1996), indicating that these two parameters are predictors of the SFI outcome. On the contrary, our results are in contrast with those obtained by Oliveira et al. (2001) who suggested that the SFI was directly correlated with nerve-fiber density and, therefore, that this parameter can be regarded as an adequate tool for evaluating sciatic functional deficiency in the rat.

Our set of histomorphometrical data can represent an important basic reference for future studies since they were obtained using a recently developed quantitative method that allows reducing the probability that systematic errors might affect results (Geuna, 2000).

The observation that, at week-8 post-operatively, the regenerated nerve fibers were still far from having reached the normal values regarding four important morphoquantitative parameters (density, number, size and myelin thickness) indicates that this post-operative time may not be appropriate to verify if (and when) the morphology of the regenerated nerves really returns to normal.

The observation that fiber density and number were increased in comparison to normal values is in accordance with previous studies on rat sciatic nerve regeneration (Mackinnon et al., 1991) which showed that these two parameters significantly increased in the first three months after nerve repair, and then slowly began to decrease. This observation is probably due to the sprouting of more than one growth cone from each severed axon leading to the presence of an abundance of regenerating axons that cross the lesion site and grow until the periphery is innervated (Mackinnon et al., 1991). The following delayed decrease in fiber density and number is due, according to the "pruning hypothesis" (Brushart et al., 1998), to the progressive death of some of the collateral fibers which did not achieve the appropriate distal target connection.

In experimental research, no general agreement has been reached so far on what is the most suitable method to test functional and morphological outcomes of nerve regeneration (Hudson et al., 2000; Munro et al., 1998). While a full recovery of the SFI was attained by week-7, other functional parameters were still recovering their original values at week-8 post-operatively. The same was true for several morphoquantitative parameters of regenerated nerve fibers suggesting that future studies need to go beyond the 8-week post-operative observation time, the usual end-point of studies on the sciatic nerve crush model. In addition, the use of multiple methods of analysis is recommended for a more global assessment of nerve regeneration and functional recovery in rat sciatic nerve crush model.

ACKNOWLEDGMENTS

We thank Dr. Goreti Coutinho for English language revision. We also thank Dr. Gertrude Beer (University Hospital, Zürich, Switzerland) for the donation of the

crushing device. This study was supported by the Portuguese Ministry of Education–PRODEP III (Educational Development Program for Portugal) and European Social Fund; and Project POSI/SRI/33574/99; and the Italian Ministry of Instruction, University and Research (MIUR).

REFERENCES

AL MOUTAERY, K., ARSHADUDDIN, M., TARIQ, M., and AL DEEB, S. (1998). Functional recovery and vitamin E level following sciatic nerve crush injury in normal and diabetic rats. Int. J. Neurosci. **96,** 245–254.

ALGORA, J., CHEN, L.E., SEABER, A.V., WONG, G.H.W., and URBANIAK, J.R. (1996). Functional effects of lymphotoxin on crushed peripheral nerve. Microsurgery **17,** 131–135.

BAIN, J.R., MACKINNON, S.E., and HUNTER, D.A. (1989). Functional evaluation of complete sciatic, peroneal, and posterior tibial nerve lesions in the rat. Plast. Reconstr. Surg. **83,** 129–136.

BARBAY, S., PEDEN, E.K., FALCHOOK, G., and NUDO, R.J. (2002). An index of topographic normality in rat somatosensory cortex: application to a sciatic nerve crush model. J. Neurophysiol. **88,** 1339–1351.

BEER, G.M., STEURER, J., and MEYER, V.E. (2001). Standardizing nerve crushes with a non-serrated clamp. J. Reconstr. Microsurg. **17,** 531–534.

BRIDGE, P.M., BALL, D.J., MACKINNON, S.E., et al. (1994). Nerve crush injuries—a model for axonotmesis. Exp. Neurol. **127,** 284–290.

BRUSHART, T.M., GERBER, J., KESSENS, P., CHEN, Y.G., and ROYALL, R.M. (1998). Contributions of pathway and neuron to preferential motor reinnervation. J. Neurosci. **18,** 8674–8681.

CARLTON, J.M., and GOLDBERG, N.H. (1986). Quantitating integrated muscle function following reinnervation. Surg. Forum **37,** 611–612.

CARRIER, L., BRUSTEIN, E., and ROSSIGNOL, S. (1997). Locomotion of the hindlimbs after neurectomy of ankle flexors in intact and spinal cats: model for the study of locomotor plasticity. J. Neurophysiol. **77,** 1979–1993.

CARRINGTON, A.L., ETTLINGER, C.B., CALCUTT, N.A., and TOMLINSON, D.R. (1991). Aldolose reductase inhibition with imirestat-effects on impulse conduction and insulin-stimulation of Na/K-adenosine triphosphatase activity in sciatic nerves of streptozotocin-diabetic rats. Diabetologia **34,** 397–401.

CHEN, L.E., SEABER, A.V., GLISSON, R.R., et al. (1992). The functional recovery of peripheral nerves following defined acute crush injuries. J. Orthop. Res. **10,** 657–664.

CHURCHILL, J.D., MUJA, N., MYERS, W.A., BESHEER, J., and GARRAGHTY, P.E. (1998). Somatotopic consolidation: a third phase of reorganization after peripheral nerve injury in adult squirrel monkeys. Exp. Brain Res. **118,** 189–196.

CLARKE, K.A., and PARKER, A.J. (1986). A quantitative study of normal locomotion in the rat. Physiol. Behav. **38,** 345–351.

CLARKE, K.A., SMART, L., and STILL, J. (2001). Ground reaction force and spatiotemporal measurements of the gait of the mouse. Behav. Res. Methods Instrum. Comput. **33,** 422–426.

CRAGG, B.G., and THOMAS, P.K. (1964). The conduction velocity of regenerated peripheral nerve fibers. J. Physiol. **171,** 164–175.

DE KONING, P., and GISPEN, W.H. (1987). Org. 2766 improves functional and electrophysiological aspects of regenerating sciatic nerve in the rat. Peptides **8,** 415–422.

DE MEDINACELI, L., FREED, W.J., and WYATT, R.J. (1982). An index of the functional condition of rat sciatic nerve based on measurements made from walking tracks. Exp. Neurol. **77,** 634–643.

DELLON, A.L., and MACKINNON, S.E. (1989). Selection of the appropriate parameter to measure neural regeneration. Ann. Plast. Surg. **23,** 197–202.

DEVOR, M., SCHONFELD, D., SELTZER, Z., and WALL, P.D. (1979). Two modes of cutaneous reinnervation following peripheral nerve injury. J. Comp. Neurol. **185,** 211–220.

DOETSCH, G.S., HARRISON, T.A., MACDONALD, A.C., and LITAKER, M.S. (1996). Short-term plasticity in primary somatosensory cortex of the rat: rapid changes in magnitudes and latencies of neuronal responses following digit dennervation. Exp. Brain Res. **112,** 505–512.

DORFMAN, L.J. (1990). Quantitative clinical electrophysiology in the evaluation of nerve injury and regeneration. Muscle Nerve **13,** 822–828.

DUPONT, E., CANU, M.H., LANGLET, C., and FALEMPIN, M. (2001). Time course of recovery of the somatosensory map following hindpaw sensory deprivation in the rat. Neurosci. Lett. **309,** 121–124.

GEUNA, S., TOS, P., BATTISTON, B., and GUGLIELMONE, R. (2000). Verification of the two-dimensional disector, a method for the unbiased estimation of density and number of myelinated nerve fibers in peripheral nerves. Ann. Anat. **182,** 23–34.

GEUNA, S. (2000). Appreciating the difference between design-based and model-based sampling strategies in quantitative morphology of the nervous system. J. Comp. Neurol. **427,** 333–339.

GEUNA, S., TOS, P., BATTISTON, B., GUGLIELMONE, R., and GIACOBINI-ROBECCHI, M.G. (2001). Methodological issues in size estimation of myelinated nerve fibers in peripheral nerves. Anat. Embryol. **204,** 1–10.

GEUNA, S., GIGO-BENATO, D., and DE CASTRO RODRIGUES, A. (2004). On sampling and sampling errors in histomorphometry of peripheral nerve fibers. Microsurgery **24,** 72–76.

GUDEMEZ, E., OZER, K., CUNNINGHAM, B., SIEMIONOW, K., BROWNE, E., and SIEMIONOW, M. (2002). Dehydroepiandrosterone as an enhancer of functional recovery following crush injury to rat sciatic nerve. Microsurgery **22,** 234–241.

HADLOCK, T., KOKA, R., VACANTI, J.P., and CHENEY, M.L. (1999). A comparison of assessments of functional recovery in the rat. J. Periph. Nerv. Syst. **4,** 258–264.

HADLOCK, T.A., SUNDBACK, C.A., HUNTER, D.A., VACANTI, J.P., and CHENEY, M.L. (2001). A new artificial nerve graft containing rolled schwann cell monolayers. Microsurgery **21,** 96–101.

HARE, G.M.T., EVANS, P.J., MACKINNON, S.E., et al. (1992). Walking track analysis: a long-term assessment of peripheral nerve recovery. Plast. Reconstr. Surg. **89,** 251–258.

HOWARD, C.S., BLAKENEY, D.C., MEDIGE, J., MOY, O.J., and PEIMER, C.A. (2000). Functional assessment in the rat by ground reaction forces. J. Biomech. **33,** 751–757.

HRUSKA, R.E., KENNEDY, S., and SILBERGELD, E.K. (1979). Quantitative aspects of normal locomotion in rats. Life Sci. **25,** 171–180.

HU, D., HU, R., and BERDE, C.B. (1997). Neurologic evaluation of infant and adult rats before and after sciatic nerve blockade. Anesthesiology **86,** 957–965.

HUDSON, T.W., EVANS, G.R., and SCHMIDT, C.E. (2000). Engineering strategies for peripheral nerve repair. Orthop. Clin. North Am. **31,** 485–497.

IJKEMA-PAASSEN, J., MEEK, M.F., and GRAMSBERGEN, A. (2001). Muscle differentiation after sciatic nerve transection and reinnervation in adult rats. Ann. Anat. **183,** 369–377.

ISLAMOV, R.R., HENDRICKS, W.A., JONES, R.J., LYALL, G.L., SPANIER, N.S., and MURASHOV, A.K. (2002). 17β-Estradiol stimulates regeneration of sciatic nerve in female mice. Brain Res. **943,** 283–286.

KANAYA, F., FIRREL, J., TSAI, T.M., and BREIDENBACH, W.C. (1992). Functional results of vascularized versus nonvascularized nerve grafting. Plast. Reconstr. Surg. **89,** 924–930.

KANAYA, F., FIRRELL, J.C., and BREIDENBACH, W.C. (1996). Sciatic function index, nerve conduction tests, muscle contraction, and axon morphometry as indicators of regeneration. Plast. Reconstr. Surg. **98,** 1264–1271.

KERNS, J.M., BRAVERMAN, B., MATHEW, A., LUCCHINETTI, C., and IVANKOVICH, A.D. (1991). A comparison of cryoprobe and crush lesions in the rat sciatic nerve. Pain **47,** 31–39.

KINGERY, W.S., and VALLIN, J.A. (1989). The development of chronic mechanical hyperalgesia, autotomy and collateral sprouting following sciatic nerve section in rat. Pain **38,** 321–332.

KINGERY, W.S., LU, J.D., ROFFERS, J.A., and KELL, D.R. (1994). The resolution of neuropathic hyperalgesia following motor and sensory functional recovery in sciatic axonotmetic mononeuropathies. Pain **58,** 157–168.

KOKA, R., and HADLOCK, T.A. (2001). Quantification of functional recovery following rat sciatic nerve transection. Exp. Neurol. **168,** 192–195.

LANGLET, C., CANU, M.H., VILTART, O., SEQUEIRA, H., and FALEMPIN, M. (2001). Hypodynamia-hypokinesia induced variations in expression of fos protein in structures related to somatosensory system in the rat. Brain Res. **29,** 72–80.

LEARDINI, A., and O'CONNOR, J.J. (2002). A model for lever-arm length calculation of the flexor and extensor muscles at the ankle. Gait Posture **15,** 220–229.

LEE, M., DOOLABH, V.B., MACKINNON, S.E., and JOST, S. (2000). FK506 promotes functional recovery in crushed rat sciatic nerve. Muscle Nerve **23,** 633–640.

LUNDBORG, G., and DAHLIN, L. (1992). The pathophysiology of nerve compression. Hand Clin. **8,** 215–227.

MACKINNON, S.E., HUDSON, A.R., and HUNTER, D.A. (1985). Histologic assessment of nerve regeneration in the rat. Plast. Reconstr. Surg. **75,** 384–388.

MACKINNON, S.E., DELLON, A.L., and O'BRIEN, J.P. (1991). Changes in nerve fiber numbers distal to a nerve repair in the rat sciatic nerve model. Muscle Nerve **14,** 1116–1122.

MADORSKY, S.J., SWETT, J.E., and CRUMLEY, R.L. (1998). Motor versus sensory neuron regeneration through collagen tubules. Plast. Reconstr. Surg. **102,** 430–436.

MASTERS, D.B., BERDE, C.B., DUTTA, S.K., et al. (1993). Prolonged regional nerve blockade by controlled release of local anesthetic from a biodegradable polymer matrix. Anesthesiology **79,** 340–346.

MUNRO, C.A., SZALAI, J.P., MACKINNON, S.E., and MIDHA, R. (1998). Lack of association between outcome measures of nerve regeneration. Muscle Nerve **21,** 1095–1097.

NAVARRO, X., and KENNEDY, W.R. (1989). Sweat gland reinnervation by sudomotor regeneration after different types of lesions and graft repairs. Exp. Neurol. **104,** 229–234.

NAVARRO, X., VERDÚ, E., and BUTÍ, M. (1994). Comparison of regenerative and reinnervation capabilities of different functional types of nerve fibers. Exp. Neurol. **129,** 217–224.

OLIVEIRA, E.F., MAZZER, N., BARBIERI, C.H., and SELLI, M. (2001). Correlation between functional index and mor-

phometry to evaluate recovery of the rat sciatic nerve following crush injury: experimental study. J. Reconstr. Microsurg. **17,** 69–75.

PAKKENBERG, B., and GUNDERSEN, H.J. (1997). Neocortical neuron number in humans: effect of sex and age. J. Comp. Neurol. **384,** 312–320.

PAYDARFAR, J.A., and PANIELLO, R.C. (2001). Functional study of four neurotoxins as inhibitors of post-traumatic nerve regeneration. Laryngoscope **111,** 844–850.

PU, L.L., SYED, S.A., REID, M., et al. (1999). Effects of nerve growth factor on nerve regeneration through a vein graft across a gap. Plast. Reconstr. Surg. **104,** 1379–1385.

RADEVIK, B., and LUNDBORG, G. (1977). Permeability of intraneural microvessels and perineurium following acute, graded experimental nerve compression. Scand. J. Plast. Reconstr. Surg. **11,** 179–187.

REMPEL, D., DAHLIN, L., and LUNDBORG, G. (1999). Pathophysiology of nerve compression syndromes: response of peripheral nerves to loading. J. Bone Joint Surg. Am. **81A,** 1600–1610.

SANES, J.N., SUNER, S., and DONOGHUE, J.P. (1990). Dynamic organization of primary cortex output to target muscles in adult rats. I. Long-term patterns of reorganization following motor or mixed peripheral nerve lesions. Exp. Brain Res. **79,** 479–491.

SCHMITZ, C. (1998). Variation of fractionator estimates and its prediction. Anat. Embryol. **198,** 371–397.

SEDDON, H. (1943). Three types of nerve injury. Brain **66,** 237–288.

SHEN, N., and ZHU, J. (1995). Application of sciatic functional index in nerve functional assessment. Microsurgery **16,** 552–555.

SPOREL-OZAKAT, R.E., EDWARDS, P.M., HEPGUL, K.T., SAVAS, A., and GISPEN, W.H. (1991). A simple method for reducing autotomy in rats with peripheral nerve lesions. J. Neurosci. Methods **36,** 263–265.

STRASBERG, S.R., WATANABE, O., MACKINNON, S.E., TARASIDIS, G., HERTL, M.C., and WELLS, M.R. (1996). Wire mesh as a post-operative physiotherapy assistive device following peripheral nerve graft repair in the rat. J. Periph. Nerv. Syst. **1,** 73–76.

SUNDERLAND, S. (1951). A classification of peripheral nerve injuries producing loss of function. Brain **78,** 491–516.

SUNDERLAND, S. (1990). The anatomy and physiology of nerve injury. Muscle Nerve **13,** 771–784.

THALHAMMER, J.G., VLADIMIROVA, M., BERSHADSKY, B., and STRICHARTZ, G.R. (1995). Neurologic evaluation of the rat during sciatic nerve block with lidocaine. Anesthesiology **82,** 1013–1025.

VALERO-CABRÉ, A., and NAVARRO, X. (2001). H reflex restitution and facilitation after different types of peripheral nerve injury and repair. Brain Res. **919,** 302–312.

VAN MEETEREN, N.L.U., BRAKKEE, J.H., HAMERS, F.P.T., HELDERS, P.J.M., and GISPEN, W.H. (1997). Exercise training improves functional recovery and motor nerve conduction velocity after sciatic nerve crush lesion in the rat. Arch. Phys. Med. Rehabil. **78,** 70–77.

VAREJÃO, A.S.P., CABRITA, A.M., PATRICIO, J.A., et al. (2001a). Functional assessment of peripheral nerve recovery in the rat: gait kinematics. Microsurgery **21,** 383–388.

VAREJÃO, A.S.P., MEEK, M.F., FERREIRA, A.J., PATRICIO, J.A., and CABRITA, A.M. (2001b). Functional evaluation of peripheral nerve regeneration in the rat: walking track analysis. J. Neurosci. Methods **108,** 1–9.

VAREJÃO, A.S.P., CABRITA, A.M., MEEK, M.F., et al. (2002). Motion of the foot and ankle during the stance phase in rats. Muscle Nerve **26,** 630–635.

VAREJÃO, A.S.P., CABRITA, A.M., GEUNA, S., FILIPE, V.M., GRAMSBERGEN, A., and MEEK, M.F. (2003a). Toe out angle: a functional index for the evaluation of sciatic nerve recovery in the rat model. Exp. Neurol. **183,** 695–699.

VAREJÃO, A.S.P., CABRITA, A.M., MEEK, M.F., et al. (2003b). Ankle kinematics to evaluate functional recovery in crushed rat sciatic nerve. Muscle Nerve **27,** 706–714.

WALKER, J.L., EVANS, J.M., MEADE, P., RESIG, P., and SISKEN, B.F. (1994a). Gait-stance duration as measure of injury and recovery in the rat sciatic nerve model. J. Neurosci. Methods **52,** 47–52.

WALKER, J.L., RESIG, P., GUARNIERI, S., SISKEN, B.F., and EVANS, J.M. (1994b). Improved footprint analysis using video recording to assess functional recovery following injury to the rat sciatic nerve. Restor. Neurol. Neurosci. **6,** 189–193.

WELLS, M.R., KRAUS, K., BATTER, D.K., et al. (1997). Gel matrix vehicles for growth factor application in nerve gap injuries repaired with tubes: a comparison of biomatrix, collagen, and methylcellulose. Exp. Neurol. **146,** 395–402.

WESTERGA, J., and GRAMSBERGEN, A. (1990). The development of locomotion in the rat. Dev. Brain Res. **57,** 163–174.

Address reprint requests to:
Artur S.P. Varejão, D.V.M., Ph.D.
Department of Veterinary Sciences
University of Trás-os-Montes e Alto Douro
P.O. Box 1013
5001-911 Vila Real, Portugal

E-mail: avarejao@utad.pt